ADSORPTION AND DIFFUSION OF CARBON DIOXIDE IN PHENOLIC RESIN CARBONIZATES

Frantisek KOLAR[a1], Pavel FOTT[b] and Jaroslava SVITILOVA[a]

[a] *Institute of Rock Structure and Mechanics, Academy of Sciences of the Czech Republic, 182 09 Prague 8, Czech Republic; e-mail:* [1] *IRSM@site.cas.cz*

[b] *Czech Hydrometeorological Institute, 143 06 Prague 4, Czech Republic*

Received April 18, 1996
Accepted June 24, 1996

The adsorption and diffusion of CO_2 in phenolic resin carbonizates prepared at final carbonization temperatures of 500, 600, and 700 °C were investigated at 20 °C and pressures of 6 to 130 kPa. The experimental data were compared with theoretical dependences obtained by numerical solution of differential equations set up based on the occluded gas model and on the model of diffusion through a pore network. The former model, which assumes that the diffusion is driven by the concentration gradient of the gas dissolved in the solid, was found to fit the experimental data better than the latter model.

Key words: Adsorption; Diffusion; Microporous carbon membranes.

Phenol formaldehyde resins are routinely used as glassy carbon precursors. Compact polymeric bodies of required shapes can be prepared from the fluid resins by gradual curing starting from the gel stage. Glassy carbon, which is thermally resistant and chemically stable and exhibits a very low porosity, can be prepared by subsequent carbonization at 1 000 °C (refs[1–3]). Such material is well suited to the manufacture of crucibles, prosthetic materials and carbon electrodes[4,5].

Glassy carbon is virtually impermeable to gases. The properties of the carbonized matter, however, depend on the conditions of preparation. The final heat treatment temperature (HTT) plays a dominant role in this. Microporous material possessing the character of molecular sieves[6,8–10] is obtained within the region of HTT = 500 to 800 °C. Porosity increases with temperature to reach its maximum at HTT about 750 °C. Such materials can in principle be employed for the manufacture of selective membranes for the separation of gases. The first authors to test the feasibility of using such microporous material as a membrane were Bird and Trimm[11]. The authors measured the diffusivity in a Wicke–Kalenbach cell for plate-shaped membranes 1.5 mm thick, carbonized up to 700 °C at a rate of 7 K/min. The results failed to provide unambiguous evidence that the membrane possessed the nature of a molecular sieve. The permselectivities were lower than as expected, and the temperature dependence did not always correspond to activated diffusion. Such behaviour was explained in terms of the occur-

rence of cracks and larger pores, which presumably enabled a parallel gas flow beyond the microporous system. Apparently, this was due to a too fast carbonization because the so-called critical heating rate[12,13] for the membrane of the given thickness was exceeded substantially.

A true selective carbon membrane possessing properties corresponding to microporous molecular sieves has been demonstrated by Koresh and Sofer[8]. This was a thin-walled capillary membrane prepared by controlled carbonization of a capillary membrane made of an unspecified polymer. Activated membranes obtained by carbonization up to 800 °C or 900 °C exhibited a high permselectivity of the O_2–N_2 pair. Subsequent studies by those authors[10] were primarily aimed at determining the dependence of the permeabilities of methane and hydrogen on the final membrane carbonization temperature. The two papers cited brought evidence that the properties of the membranes can be modified by suitably adjusting the preparation conditions, particularly the final carbonization temperature, perhaps in combination with gentle activation.

Hatori and coworkers[9,14] described the preparation of carbon membranes by carbonization of polyimides of the Kapton type at 800 °C. This material exhibits a high permeability for CO_2 (even higher than for He), which suggests that the transport mechanism can rest in activated diffusion or diffusion in micropores. Analogous behaviour which can be explained in terms of the solution-diffusion mechanism has been reported for a number of polymeric membranes[15,16].

Our previous study[6] dealt in particular with the development of the microporous structure and with the transport properties of materials carbonized up to different HTTs. The transport properties were evaluated based on observed water vapour sorption kinetics for plate-shaped test bodies usually 2 mm thick. This approach allowed us to examine the relationship between the microporosity and transport properties and to find the optimum HTT for the preparation of the membranes. However, we failed to identify reliably the adequate diffusion model.

The present work addresses the diffusion mechanism problem, with the aim to identify the predominant driving forces of diffusion in microporous carbon materials. Adsorption isothermal experiments were performed in a constant-volume apparatus enabling us to investigate both the kinetic and equilibrium characteristics (diffusivity, sorption isotherm parameters). Carbon dioxide was chosen as the sorbate because this gas is sorbed in the carbonizates to a sufficient extent at room temperature and its sorption isotherm is markedly concave, which is a prerequisite for selecting the appropriate diffusion model[6,10]. Based on the results, two feasible driving forces were considered:

a) the concentration gradient of the gas “dissolved” in the solid, as is the case in polymeric membranes or zeolites,

b) the partial gas pressure gradient, as is the case for Knudsen’s diffusion in mesopores.

THEORETICAL

With respect to their diameter, pores are classed (IUPAC) as macropores ($r > 25$ nm), mesopores ($1 < r < 25$ nm), or micropores ($r < 1$ nm). In the permeation of gases through the membrane, each type of pore is associated with a different kind of gas flow. Nonselective viscous flow is predominant in macropores. Knudsen's flow prevails in mesopores, where the mean free path of the diffusing molecules is longer than the pore diameter, so that impacts of molecules on the wall are more frequent than mutual collisions. And two models are feasible to describe the migration of gases in microporous systems, viz. the occluded gas model and the model of gas diffusion in pores[17,18], as described below.

Occluded Gas Model

In this model it is assumed that the gas is dissolved in the solid. This approach is conventionally applied to the description of diffusion in polymers and carbon-based or zeolitic molecular sieves[17,18,24]. Constant transport pores need not necessarily exist in this model. In the non-porous body the gas migrates by true diffusion, the process being associated with molecular jumps[19]. The transport is driven by the concentration gradient $\mathrm{d}C/\mathrm{d}x$ where concentration C is taken with respect to the volume unit of the body bulk. The validity of Fick's law for the gas flow N is assumed in the form

$$N = -D_s \, \mathrm{d}C/\mathrm{d}x \quad , \tag{1}$$

where D_s is the corresponding diffusion coefficient.

Model of Diffusion in Pores

In this case the gas transport occurs through a network of pores and is driven by the gradient $\mathrm{d}C_g/\mathrm{d}x$, where C_g is the gas concentration with respect to the pore volume. For an ideal gas, $C_g = p/RT$, where p is the gas pressure. Fick's law then takes the form[17,18]

$$N = -D_g \, \mathrm{d}C_g/\mathrm{d}x \quad , \tag{2}$$

where D_g is the diffusion coefficient corresponding to the model in question.

In principle, transport by both mechanisms simultaneously is possible. The predominance of one of them can be ascertained based on the diffusivity values measured at different pressures. The following equation is then employed:

$$D_g = RTD_s \, \mathrm{d}C/\mathrm{d}p \quad , \tag{3}$$

which is obtained by combining the diffusion flow equations (*1*) and (*2*).

For a nonlinear isotherm the experimental diffusivities cannot refer to both models simultaneously. If the observed data are evaluated by one of them, the diffusivities corresponding formally to the other model can be calculated by Eq. (*3*). If the diffusion obeys the corresponding Fick's law, then in the adequate model the diffusivities are pressure independent.

EXPERIMENTAL

Foils 0.1 mm thick were prepared by thermal curing of the resol resin Umaform F catalyzed by *p*-toluenesulfonic acid. The material was first allowed to polymerize at 60 °C for 24 h. The gelated semiproduct was removed from the mould and cut to platelets about 8 mm × 20 mm in size, which were aftercured at 90 °C for 4 h and then at 150 °C for 2 h. So prepared, the resit platelets were carbonized under nitrogen to the final HTT of 500, 600, or 700 °C applying a heating rate of 100 °C/h. According to refs[6,7,12], open microporosity develops appreciably at such HTTs. For platelets 0.1 mm thick, the heating rate of 100 °C/h is deeply below the critical rate at which the material starts to be damaged[12,13].

The bulk density of the samples was determined by the modified hydrostatic method[6].

Adsorption measurements were performed on a Carlo Erba Sorptomatic 180 apparatus using carbon dioxide as the adsorbate at 20 °C and pressures of 6 to 130 kPa. The instrument was adapted to allow the time behaviour of pressure in the adsorption vessel to be monitored continuously from the start as far as the establishment of equilibrium. The sample weight (2 to 3 g) was chosen so that the entire isotherm should involve about 10 points (i.e. 10 dose additions). The samples were evacuated at 180 °C for 8 h prior to measurement. A typical time development of pressure in the adsorption vessel is shown in Fig. 1. The starting pressure was calculated based on the equation of state of an ideal gas and using the constants of the apparatus following ref.[20]. The calculated value of the initial pressure was invariably somewhat higher than the peak top because partial adsorption took place as early as the travel of the plunger.

RESULTS AND DISCUSSION

The equilibrium pressures $p_r^{(i)}$ were measured for all injection cycles (the superscript (i) is the serial number of the injection). The equilibrium molar concentration of the gas sorbed in the sample after the i-th injection, $C_r^{(i)}$, was calculated based on Eq. (*4*) which follows from the ideal gas balance,

$$C_r^{(i)} = C_r^{(i-1)} + \frac{Q^{(i)}}{V_s} - \frac{p_r^{(i)} - p_r^{(i-1)}}{RT} \frac{V}{V_s} \,, \qquad (4)$$

where $Q^{(i)}$ is the gas dose (mol), R is the molar gas constant, T is the absolute temperature, V is the gas volume in the adsorption vessel, and V_s is the sample volume.

In the dose calculation, correction was made for the void volume of the proportioning device, and the so-called effective temperature was introduced (see ref.[20]).

The experimental data are well fitted by the Dubinin–Radushkevich equation, modified for concentration C_r as

$$C_r = C_r^{(\infty)} \exp\left[-\left(\frac{RT}{E} \ln \frac{f_r^{(\infty)}}{f_r} \right)^2 \right], \qquad (5)$$

where f_r is the fugacity corresponding to pressure p_r.

Since the pressures were very low, we put $f_r = p_r$. Fugacity $f_r^{(\infty)}$ was calculated from the saturated pressure of CO_2 ($p_r^{(\infty)}$ = 6.4326 MPa) by multiplication by the fugacity coefficient γ = 0.7314 (ref.[21]). The characteristic energy E and concentration $C_r^{(\infty)}$ corresponding to $f_r^{(\infty)}$ were determined by nonlinear regression. The adsorption isotherms of the carbonizates studied are shown in Fig. 2.

The mean pore diameter $\bar{r}$, the most probable pore diameter r_{mode}, the micropore surface area S_{micro}, and the porosity ε were calculated by the procedure reported by

TABLE I
Equilibrium characteristics of carbonizates C500, C600, and C700

Constant	C500	C600	C700
ρ_b, kg m^{-3}	1 190	1 230	1 400
$C_r^{(\infty)}$, mol m^{-3}	4 321.15	6 259.38	7 963.05
E, J mol^{-1}	9 949.70	10 071.75	10 338.79
ε, vol.%	23.09	30.80	39.41
$\bar{r}$, nm	0.734	0.731	0.725
r_{mode}, nm	0.664	0.661	0.655
S_{micro}, m^2 kg^{-1}	4.90 . 10^5	6.89 . 10^5	7.77 . 10^5

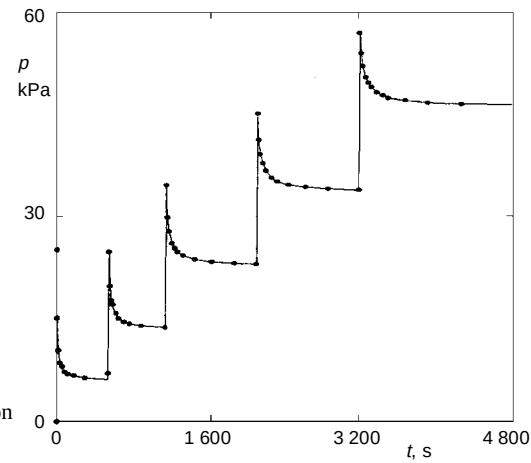

FIG. 1
Typical pressure behaviour in the adsorption vessel for sample C600

Medek[22]. The results are given in Table I. The data show that the micropore volume increases with increasing carbonization temperature over the region of 500–700 °C, whereas the pore size does not change appreciably. It should be borne in mind, however, that the pore size was calculated from the equilibrium parameters of the Dubinin–Radushkevich equation, and the values so obtained refer to the dimensions of the internal pore cavities rather than the dimensions of the pore openings, which grow narrower during the carbonization process and ultimately close completely[1,6].

The time dependences of pressure $p^{(i)}(t)$ obtained during the CO_2 sorption measurements were evaluated based on Fick's law. A similar calculation has been performed in ref.[23], dealing with the diffusion in zeolites, for a body of a spherical shape. In our case the shape of the samples allowed the gas transport to be described by means of the diffusion equation for an infinite plate, viz.

$$\frac{\partial C^{(i)}}{\partial t} = D_s \frac{\partial^2 C^{(i)}}{\partial x^2} \quad . \tag{6}$$

Assume that the diffusion coefficient D_s is independent of both the spatial coordinates and the gas concentration. In view of the symmetry of the problem, it is sufficient to solve the equation for one-half of the body. The starting condition is considered in the form

$$C^{(0)}(x,0) = 0$$

$$C^{(i)}(x,0) = C_r^{(i-1)} \qquad 0 < x < L \qquad i = 1, 2, \ldots \tag{7}$$

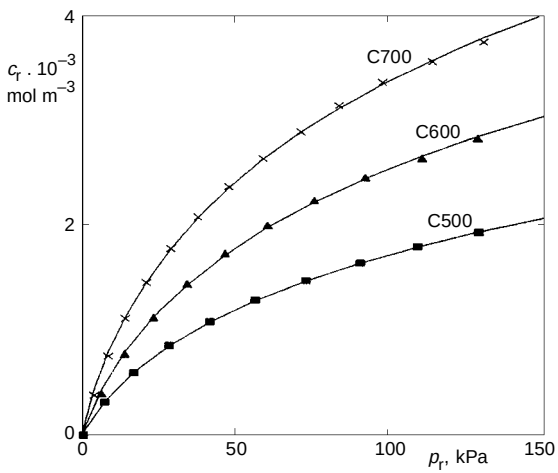

FIG. 2
Adsorption isotherms of carbon dioxide for carbonizates C500, C600, and C700; curves calculated from Eq. (*7*)

where L is the plate half thickness.

The boundary conditions will be based on the assumption that the gas sorption on the surface is much faster than the subsequent diffusion into the bulk. Hence, the surface concentration will be in equilibrium with the ambient pressure (p) during whole process:

$$C^{(i)}(L,t) = C_r(p^{(i)}) \quad t > 0 \ , \tag{8}$$

where C_r is the corresponding isotherm.

The condition for $x = 0$ is obviously

$$\left(\frac{\partial C^{(i)}}{\partial x}\right)_{x=0} = 0 \ . \tag{9}$$

The following equation can be derived for the instantaneous pressure in the adsorption vessel:

$$p^{(i)} = p_r^{(i-1)} + \frac{RT}{V}\left[Q^{(i)} + V_s(C_r^{(i)} - \overline{C}^{(i)})\right] \ , \tag{10}$$

where $\overline{C}^{(i)}$ is the mean concentration, given by the integral

$$\overline{C}^{(i)} = \frac{1}{L}\int_0^L C^{(i)}\,\mathrm{d}x \ . \tag{11}$$

The diffusion equation (*6*) was solved numerically by the network method. The modified Dubinin–Radushkevich isotherm (*5*) was chosen as the boundary condition. The diffusion coefficients D_s were determined by nonlinear regression based on the minimization of squares of differences between the observed and calculated pressures for each injection cycle separately. A typical time development of pressure (response to dose addition) for the carbonizate C600 is shown in Fig. 1. The experimental points are fitted by the calculated $p(i) = f(t)$ curves.

The calculated diffusivities are given in Tables II–IV. The optimized diffusion coefficients are identical for all the injection cycles within an error not exceeding 10%. Thus the D_s value can be regarded as pressure independent for all the carbonizates tested. The diffusivity attains its maximum at HTT = 600 °C, whereas the porosity of the carbonizates increases with increasing carbonization temperature as far as HTT = 700 °C. This is consistent with the results published for the diffusion of water vapour in carbonizates[6]. This apparent anomaly (decrease in diffusivity with increasing poros-

ity) can be explained in terms of the pore openings being closed. The porosity of the micropores corresponds to the volume of the pore cavities, while the diffusion is controlled by the diameter of the pore openings.

Equation (*3*) was used to calculate the diffusion coefficients for the model of diffusion in pores, D_g, for all injection cycles (see Tables II–IV). The D_g values are seen to decrease with increasing pressure. In Fig. 3, the D_g values are plotted against the mean pressure in the injection cycle $\bar{p} = (p_{max} + p_r)/2$, where p_{max} is the pressure corresponding to the dose injected. The points are fitted by the function $D_s\, dC_r/dp$, where $C_r(p)$ are the corresponding Dubinin sorption isotherms. The results suggest that the occluded gas model fits the experimental data better than the model of diffusion in pores, as is the case with polymeric membranes[15,16] and zeolite molecular sieves[24] (the so-called solu-

TABLE II
Diffusion characteristics of carbonizate C500

Cycle No.	p_r, kPa	p_{max}, kPa	$D_s \cdot 10^5$, $m^2\ s^{-1}$	$D_g \cdot 10^4$, $m^2\ s^{-1}$
1	7.20	31.05	0.90	5.25
2	16.67	38.20	1.05	5.07
3	28.13	47.60	0.99	3.97
4	41.33	58.98	0.89	2.98
5	56.26	72.09	1.24	3.51
6	72.79	86.91	1.07	2.59
7	90.52	103.32	1.16	2.42

$\overline{D_s} = 1.04 \cdot 10^{-5} \pm 9.89 \cdot 10^{-7}\ m^2\ s^{-1}$.

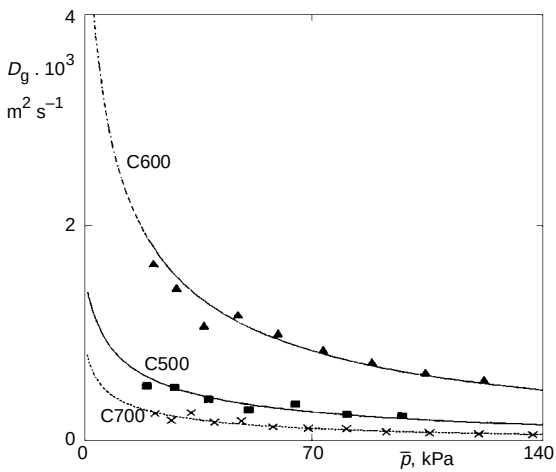

FIG. 3
Decrease of the diffusion coefficient D_g with increasing pressure

tion-diffusion mechanism). Koresh and Sofer[10] also applied the occluded gas model to the description of the steady-state permeation data for microporous carbon materials.

The gas transport through the membrane is also related to the rate of diffusion. Gas migration comprises its sorption on the membrane surface, diffusion through the membrane, and desorption on the other side of the membrane. In the steady state, the gas flow through the membrane (N) can be described by means of permeability P as

$$N = P \frac{(p_0 - p_1)}{2L} \quad , \tag{12}$$

TABLE III
Diffusion characteristics of carbonizate C600

Cycle No.	p_r, kPa	p_{max}, kPa	$D_s \cdot 10^5$, $m^2\ s^{-1}$	$D_g \cdot 10^4$, $m^2\ s^{-1}$
1	6.13	30.89	2.00	16.55
2	13.60	36.92	2.03	14.30
3	22.80	44.32	1.80	10.82
4	33.60	53.44	2.30	11.78
5	46.00	64.16	2.30	10.08
6	59.99	76.46	2.27	8.56
7	75.19	90.34	2.28	7.45
8	91.72	105.42	2.27	6.48
9	110.26	121.81	2.32	5.82

$\overline{D_s} = 2.17 \cdot 10^{-5} \pm 1.54 \cdot 10^{-6}\ m^2\ s^{-1}$.

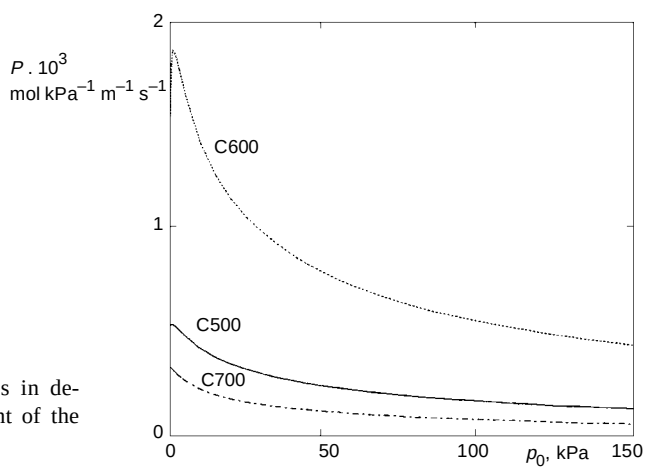

FIG. 4
Permeability of the carbonizates in dependence on the pressure in front of the membrane

where p_0 and p_1 are the pressures in front of and behind the membrane.

The rate of permeation is governed by the slowest step, which is diffusion, while the sorption on the membrane surface and desorption from it are much faster. The following relation between the permeability and diffusivity can be easily derived:

$$P = D_s \frac{C_r(p_0) - C_r(p_1)}{p_0 - p_1} \quad , \tag{13}$$

where $C_r(p_0)$ and $C_r(p_1)$ are the surface concentrations on the front and rear sides of the membrane, respectively, determined by the corresponding isotherm.

Hence, as well as on the pressure difference on the two ends of the membrane, the permeability also depends on the shape of the sorption isotherm. For the convex Dubinin–Radushkevich isotherm, which describes the adsorption of CO_2 in the carbonizates very well[6], the permeability attains its maximum at a pressure near to zero and then decreases monotonically. For permeation of CO_2 through the membrane into a vacuum ($p_1 = 0$), the dependences of P on the pressure in front of the membrane (p_0) calculated from Eq. (*13*) are shown in Fig. 4. A decrease in permeability with increasing pressure has been observed, for instance, for CO_2 and CH_4 (ref.[17]), whereas for gases with small molecules, such as H_2 and He, permeability has been found to be pressure independent. This is consistent with the fact that the latter gases give a linear isotherm over the pressure region applied.

TABLE IV
Diffusion characteristics of carbonizate C700

Cycle No.	p_r, kPa	p_{max}, kPa	$D_s \cdot 10^5$, $m^2\ s^{-1}$	$D_g \cdot 10^4$, $m^2\ s^{-1}$
2	8.27	31.00	2.50	2.68
3	13.73	34.70	2.13	2.02
4	20.26	39.21	3.25	2.72
5	28.00	44.63	2.50	1.84
6	36.93	51.11	3.05	1.98
7	47.06	58.79	2.51	1.43
8	58.26	67.66	2.60	1.31
9	70.66	77.72	2.80	1.25
10	82.93	88.84	2.40	0.96
11	97.19	101.15	2.40	0.86
12	113.19	127.49	2.40	0.77
13	129.99	127.49	2.40	0.69

$\overline{D_s} = 2.58 \cdot 10^{-6} \pm 2.31 \cdot 10^{-7}\ m^2\ s^{-1}$.

SYMBOLS

C	gas concentration with respect to the body bulk
$\overline{C}$	mean gas concentration
C_g	gas concentration with respect to the micropore volume
$C_r^{(\infty)}$	preexponential factor in Eq. (*5*)
D_s	diffusion coefficient in the in the occluded gas model
D_g	diffusion coefficient in the model of diffusion in pores
E	characteristic energy – parameter in Eq. (*5*)
f	gas fugacity
f_r	fugacity corresponding to the saturated gas pressure
N	gas flow
L	membrane half thickness
Q	gas dose
P	permeability
p	gas pressure
p_0, p_1	gas pressures in front of and behind the membrane
R	universal gas constant
$\overline{r}$	mean pore diameter
r_{mode}	most probable pore diameter
S_{micro}	micropore surface area
T	absolute temperature
t	time
V	gas volume in the adsorption vessel
V_s	sample volume
ε	porosity
γ	fugacity coefficient
ρ_b	bulk density
Superscript	
(i)	injection serial number
Subscript	
r	equilibrium value

This research was supported by the Grant Agency of the Czech Republic, Project No. 104/94/0596.

REFERENCES

1. Fitzer E., Schafer W.: Carbon *8*, 353 (1970).
2. Lausevic Z., Marinkovic S.: Carbon *24*, 579 (1986).
3. Fitzer E., Schafer W., Yamada S.: Carbon *7*, 648 (1969).
4. Glogar P., Balik K., Kolar F., Marek J.: Acta Montana *1* (85), 83 (1992).
5. Stulik K.: Electroanalysis *4*, 829 (1992).
6. Fott P., Kolar F., Weishauptova Z.: Collect. Czech. Chem. Commun. *60*, 172 (1995).
7. Fott P., Kolar F., Weishauptova Z.: Acta Montana *3* (91), 5 (1994).
8. Koresh J. E., Sofer A.: Sep. Sci. Technol. *18* (8), 723 (1983).
9. Hatori H., Yamada Y., Shiraishi M.: Carbon *30*, 303 (1991).
10. Koresh J. E., Sofer A.: J. Chem. Soc., Faraday Trans. *82*, 2057 (1986).

11. Bird A. J., Trimm D. L.: Carbon *21*, 177 (1983).
12. Choe C. R., Lee K. H.: Carbon *30*, 247 (1992).
13. Kolar F., Fott P, Balik K.: Acta Montana *3* (91), 23 (1994).
14. Hatori H., Yamada Y., Shiraishi M., Nakata H., Yoshitomi S.: Carbon *30*, 719 (1991).
15. Paul D. R.: Ber. Bunsenges. Phys. Chem. *83*, 294 (1979).
16. Van Amerongen: Rubber Chem. Technol. *37*, 1065 (1964).
17. Walker P. L., Mahajan O. P.: *Analytical Methods of Coal and Coal Products.* Academic Press, New York 1978.
18. Walker P. L., Austin L. G.: *Chemistry and Physics of Carbon*. Dekker, New York 1966.
19. Meissner B., Zilvar V.: *Fyzika polymeru. SNTL, Praha, and Alfa, Bratislava 1987.*
20. Weishauptova Z., Medek J.: Chem. Listy *77*, 300 (1983).
21. Moore W. J.: *Fyzikalni chemie*. SNTL, Praha 1979.
22. Medek J.: Fuel *56*, 131 (1977).
23. Radeke K. H.: Z. Phys. Chem. *259*, 568 (1978).
24. Karger J., Ruthven D. M.: *Diffusion in Zeolites*. Wiley, New York 1987.